ACS Catalysis

Research Article

pubs.acs.org/acscatalysis

Toward the Electrochemical Valorization of Glycerol: Fourier Transform Infrared Spectroscopic and Chromatographic Studies

Yaovi Holade, Cláudia Morais,* Karine Servat, Teko W. Napporn, and K. Boniface Kokoh

Université de Poitiers, IC2MP CNRS UMR 7285, 4 rue Michel Brunet−B27, BP 633, 86022 Poitiers cedex, France

Supporting Information

ABSTRACT: Glycerol electrooxidation reaction has been investigated by electrochemical, spectroelectrochemical, and chromatographic methods on palladium−nickel and palladium−silver nanoparticules supported on carbon Vulcan XC 72R. These materials, prepared by the so-called "Bromide Anion Exchange" method, exhibited high activity toward the glycerol electrooxidation in alkaline medium showing furthermore an important shift of the onset potential toward low potential values. Electrolysis coupled with high-performance liquid chromatography (HPLC) and in situ Fourier transform infrared spectroscopy (FTIRS) measurements have been used to determine the various compounds generated in the oxidative conversion of this three hydroxyl groups carbon molecule. Some products with high added value such as glycerate and tartronate have been identified. In situ FTIRS results have furthermore shown the pH decrease in the thin layer near the electrode. These results will positively serve as guidelines for future works on the potential use of glycerol in fuel cell devices in a cogeneration of high value chemicals and energy process.

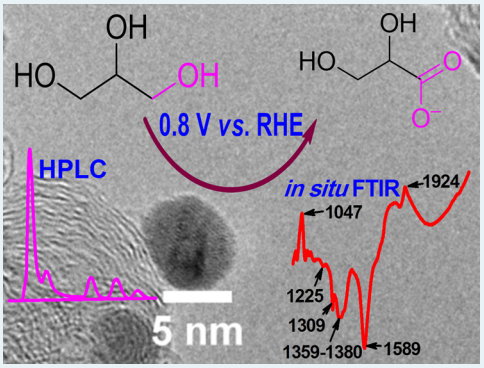

KEYWORDS: *glycerol electrooxidation, palladium-based nanoparticles, FTIR spectroelectrochemistry, bromide anion exchange, chromatographic analysis*

INTRODUCTION

Because of the depletion of fossil resources, small organic molecules became electrocatalytically attractive, making their fundamental studies in electrocatalysis an important topic.[1−5] The potential use of these molecules, principally alcohols, is of particular interest because of their potential application in direct fuel cells[6−8] and their possible chemical/industrial valorization.[9] Glycerol may be particularly interesting since its selective oxidation leads to products with high added value owing to its three hydroxyl groups.[10,11] Furthermore, since its production exceeds by far its present consumption an alternative utilization is desirable, and the possible use of glycerol in direct oxidation fuel cells appears as an interesting option. In spite of its quite low specific energy (4.4 against 6.1 kWh·kg^{-1} for methanol), glycerol is attractive compared with other fuels because it is non toxic, has a low volatility, and its transport and storage are not demanding.[12,13]

Despite these advantages, the electrocatalytic oxidation of glycerol has been less studied than other organic molecules. Nevertheless, during the past decade, some studies were devoted to glycerol oxidation in the fields of organic chemistry ($KMnO_4$, $K_2Cr_2O_7$),[14,15] heterogeneous catalysis with oxygen as oxidizing agent,[16−18] and in electrocatalysis, where the electrocatalysts showed the best activity in alkaline medium.[1,3,19] Various bimetallic electrocatalysts involving palladium and nickel, silver, gold, or platinum have shown to be electrocatalytically active toward alcohol oxidation in alkaline medium.[3,10,20−30] Palladium is of particular interest because it was shown to efficiently electrooxidize alcohols such as ethanol or glycerol as compared with platinum. Not only has Pd revealed notable anodic peak current, but the alcohol oxidation remarkably increased on the surface of the PdPt bimetallic catalyst. This enhancement of the activity in PdPt alloys was attributed to an electronic effect in which the d-band center of Pd was raised by the presence of nearby Pt.[3,31] Several authors also showed an important shift in the onset potential and a significant increase in the peak current for the alcohol oxidation on the PdAu anode materials.[30,32−34] Indeed, although Au nanoparticles may not directly lead to practically active electrocatalysts for the alcohol oxidation, they can enhance the activity of precious metal catalysts. Besides, the association of palladium and gold was shown to decrease the hydrogen absorption in the Pd network and therefore does contribute to the durability of Pd-based materials.[35] Other cocatalysts such as bismuth,[32] ruthenium,[3,4,36] and rhodium[37] were also proposed. They were shown to suitably promote a bifunctional mechanism through the formation hydroxyl ions at low potential, improving the oxidative conversion of glycerol. In particular, if the purpose is to perform thorough conversion of glycerol as fuel in a PEM system, rhodium would be an appropriate candidate as it promotes the cleavage of the C−C bonds in the glycerol molecule.[37] Nickel and silver which are very stable in alkaline medium might also be of great interest since

Received: March 19, 2013
Revised: September 9, 2013
Published: September 12, 2013

   dx.doi.org/10.1021/cs400559d | ACS Catal. 2013, 3, 2403−2411

they enable to decrease markedly the Pd amount without significantly decreasing the activity. Indeed, these cocatalysts are well-known to promote an enhancement of the performance the Pd electrode materials.[25,26,28,38−43]

Coupling electrochemical methods to analytical (chromatography, online or differential electrochemical mass spectrometry) and spectroscopic (in situ FTIR)[11,44−49] measurements permit to identify the intermediate species and the final reaction products which might be very helpful to evaluate the activity of an electrode catalyst toward an organic compound and to understand the reaction mechanism. This knowledge can also allow tailoring a catalyst composition for a selective reaction process to added value products. The judicious combination of electrochemical, spectroscopic, and chromatographic methods allows therefore to gain clear information about the electrooxidation of an organic compound such as glycerol. Recently, the combination of cyclic voltammetry measurements with HPLC and/or in situ spectroscopic techniques was reported for the study of glycerol electrooxidation.[11,30,32,46−48,50] Nevertheless there is still a lack of data about the glycerol electrooxidation reaction.

In this context, the purpose of the present work is to investigate the glycerol electrooxidation in alkaline medium on nickel and silver modified Pd anode materials synthesized by a soft and clean method. Indeed, it is well-known that the microemulsion synthesis method currently used to obtain these materials leads to catalysts with some sites inaccessible by the reactive species. The method used herein is expected to provide catalysts with high active surface areas and consequently lead to an enhancement of the oxidation current densities at lower potential values. As stated above glycerol is a renewable and sustainable organic compound which can possibly be used in a valuable chemicals and energy cogeneration approach.[10,19,30,51] For this purpose it is of great interest to provide insights on the mechanism of its electrooxidation on these PdM/C (M = Ag, Ni) nanocatalysts in alkaline medium, and this is another objective of the present study. To this aim chromatographic analysis (HPLC) and in situ FTIR spectroelectrochemistry experiments have been combined to identify both the intermediates and the final products of the glycerol oxidation process and hopefully propose a preferential pathway for this reaction.

MATERIALS AND METHODS

Nanoscale Materials Synthesis by "Bromide Anion Exchange". PdNi/C and PdAg/C catalysts with different atomic compositions have been synthesized using the "Bromide Anion Exchange" (BAE) method; first proposed for gold−platinum supported catalysts.[52] The details about this method modified for palladium−nickel and palladium−silver catalyst synthesis are reported elsewhere.[38] BAE consists of a soft and clean method which does not involve any organic compound as surfactant or stabilizer as a few other methods.[53−61] The obtained materials were characterized by different physicochemical methods, namely, differential and thermogravimetric analysis (DTA/TGA), X-ray diffraction (XRD), and Transmission Electron Microscopy (TEM). Physicochemical characterizations indicated a metal loading of about 30 wt % and particle sizes from 3 to 6 nm (Supporting Information, Table S1).

Cyclic Voltammetry (CV). CV experiments were performed by using an analogical potentiostat EG&G PARC Model 362 (Princeton Applied Research) in a conventional three-electrode cell.[62−64] A Reversible Hydrogen Electrode (RHE) and a slab of glassy carbon of 6.48 cm^2 geometrical surface area were used as reference and counter electrodes, respectively. The reference electrode was separated from the solution by a Luggin capillary tip. The working electrode consisted of a catalytic powder deposited on a glassy carbon disk used as conductive carrier with a 3 mm diameter. The catalytic ink was prepared following a procedure similar to that described by Wilson and co-workers[65] for fuel cell catalytic ink preparation using the conductive ionomer Nafion (5 wt %).[66−68] Briefly, the metal/C powder (4 mg) was added in a homogeneous mixture of 50 μL of Nafion solution (5 wt % from Sigma-Aldrich) and 375 μL of ultra pure water. Three microliters of the homogeneous catalytic ink were finally deposited with a syringe onto the freshly polished glassy carbon disk, and the solvent was evaporated in a stream of ultrapure nitrogen at room temperature. This amount of material represents 116.40 $\mu g\ cm^{-2}$ of metal loading. All the CV experiments were performed at room temperature (21 ± 1 °C) with 0.1 mol L^{-1} NaOH (Sigma-Aldrich, 97%), 0.1 mol L^{-1} glycerol (ReagentPlus >99.0%, Sigma-Aldrich), and ultrapure water (18.2 MΩ cm at 20 °C). The solution was first deoxygenated by bubbling nitrogen for 30 min before any electrochemical experiment.

Electrolysis and High-Performance Liquid Chromatography (HPLC). Electrolysis was fulfilled in a Pyrex two-compartment cell.[69] The compartments were separated with an anion-exchange membrane (35 μm thickness, from Fumatech). The electrochemical measurements were conducted using a Potentiostat (Voltalab PGZ 402 from Radiometer Analytical) which was controlled by a computer with Voltamaster 4 software. The electrical connection of the carbon Toray sheet was established with a gold wire thanks to a carbon paste. The ink was prepared like for the CV experiments. Fifty microliters of the catalytic ink were deposited onto each side of a carbon Toray sheet (1.5 cm^2 geometric surface area), and the solvent was evaporated with a N_2 stream at room temperature. A glassy carbon slab (10.8 cm^2 geometric surface area) and RHE served as counter and reference electrodes, respectively. The programmed potential electrolysis (PPE) setup consisted of two potential levels: a first potential plateau was set at E_{ox} = 0.8 V vs RHE (20 s for electrooxidation of organic molecules) and a second one fixed at E_{des} = 1.4 V vs RHE for 1 s allowed the removal of the poison species or the regeneration of the catalytic surface.

The final products of glycerol electrooxidation were determined by analyzing collected samples with high-performance liquid chromatography (Dionex system P680 HPLC). It works with an isocratic elution and mainly includes an autosampler (ASI 100 Automated Sample Injector), a sample loop (20 μL), and an ion-exclusion column (Aminex HPX-87H), which operated at room temperature. The analytes were separated with diluted sulfuric acid (3.3 mmol L^{-1} H_2SO_4, MERCK 96%) used as eluent with a 0.6 mL min^{-1} flow rate. The chromatograph was equipped with an UV−vis detector (λ = 210 nm) followed by a refractive index detector (IOTA2). The assignments of the different peaks and the quantitative determination of the products were done with external standards, that is, by comparing the retention times with those of reference samples prepared with the expected products of glycerol electrooxidation.[10,11]

In Situ Fourier Transform Infrared (FTIR) Spectroscopy Measurements Coupled with Electrochemical Experiments. In situ FTIR measurements were carried out in a Bruker IFS 66v spectrometer which was modified for beam reflection on the electrode surface at a 65° incidence angle. A 10^{-6} bar vacuum

dx.doi.org/10.1021/cs400559d | ACS Catal. 2013, 3, 2403−2411

was used to remove all interferences from atmospheric water and CO_2. The detector was a MCT (HgCdTe) type, cooled beforehand by liquid nitrogen. The spectral resolution was 4 cm^{-1}, and the FTIR spectra were recorded in the 1000 cm^{-1} and 4000 cm^{-1} IR region. A special tailored cell, in a three-electrode spectroelectrochemical cell, fitted with an MIR transparent window (CaF_2) was used for in situ FTIR experiments.[70−72] The potentiostat was the same used in CV experiments. A slab of glassy carbon and RHE served as counter and reference electrodes, respectively. The working electrode consisted of 3 μL of catalytic ink deposited on a glassy carbon disk (8 mm diameter). To minimize the absorption of the infrared beam by the solution, the working electrode was pressed against the window and a thin layer of electrolytic solution was obtained. Two methods were used. The first one was the SPAIRS (Single Potential Alteration IR Spectroscopy), carried out in the potential range of 0.3−1.45 V vs RHE. The electrode reflectivity R_{Ei} was recorded at different potentials E_i, each separated by 0.05 V during the first voltammogram at a sweep rate of 1 mV s^{-1}. The second spectroelectrochemical method was a Chronoamperometry/FTIRS coupling which was performed at 0.8 V vs RHE for 1 h with a spectrum acquisition every 3 min.

RESULTS AND DISCUSSION

Electrochemical Characterization of the Catalysts. The electrochemical characterization of the catalysts was performed by CV experiments in a N_2-satured 0.1 mol L^{-1} NaOH solution. Figure 1a shows the cyclic voltammograms of PdNi/C catalysts. The lower potential limit has been set to 0.30 V vs RHE to avoid the irreversible insertion of hydrogen in the palladium crystal lattice.[73,74] During the positive-direction scan, the hydrogen desorption occurs at about 0.59 V vs RHE (peak A_1), and the palladium surface oxidation takes place at about 0.70 V vs RHE (peak A_2). The reduction of PdO occurs during the backward scan between 0.55 and 0.50 V vs RHE, depending on the nickel content in the catalyst composition (peak A_3). The upper potential limit was set to 1.6 V vs RHE for Ni containing materials to see the NiOOH formation peak at about 1.5 V vs RHE (peak B_1) and the corresponding reduction peak (B_2) occurring during the negative-direction sweep. Figure 1b shows steady-state cyclic voltammograms of PdAg/C nanocatalysts. Peak C_1 is due to the Ag_2O reduction, and peak C_2 is attributed to palladium oxide reduction. It should be noted that when the silver atomic composition is lower than or equal to 50%, the intensity of peak C_1 (Ag_2O reduction) decreases with cycling and disappears after 20 cycles. This behavior was already reported for PdAg/C catalysts and attributed to a surface rearrangement which can be due to either its enrichment in Pd or to the dissolution of the Ag species when setting the upper potential limit to 1.6 V vs RHE.[21,28,75] To exclude the latter hypothesis the bulk electrolyte solution was analyzed, and no dissolved metal species like Ag^+ were found.[38] Furthermore, a careful comparison of the shape of cyclic voltammograms obtained for monometallic Pd/C and bimetallic PdAg/C materials at high potential values indicates the presence of silver in the catalyst, supporting therefore the first hypothesis of the migration of Pd atoms to the surface without Ag dissolution. As an additional proof, we provide cyclic voltammogram of $Pd_{30}Ag_{70}/C$ in 0.1 mol L^{-1} at 50 mV s^{-1} (Supporting Information, Figure S1). Indeed, when the silver atomic composition is higher than 50% in the PdAg/C materials the reduction peaks of Ag_2O do not disappear, remaining stable after 22 complete cyclic voltammograms. The active surface area of Pd/C catalyst was evaluated by integrating

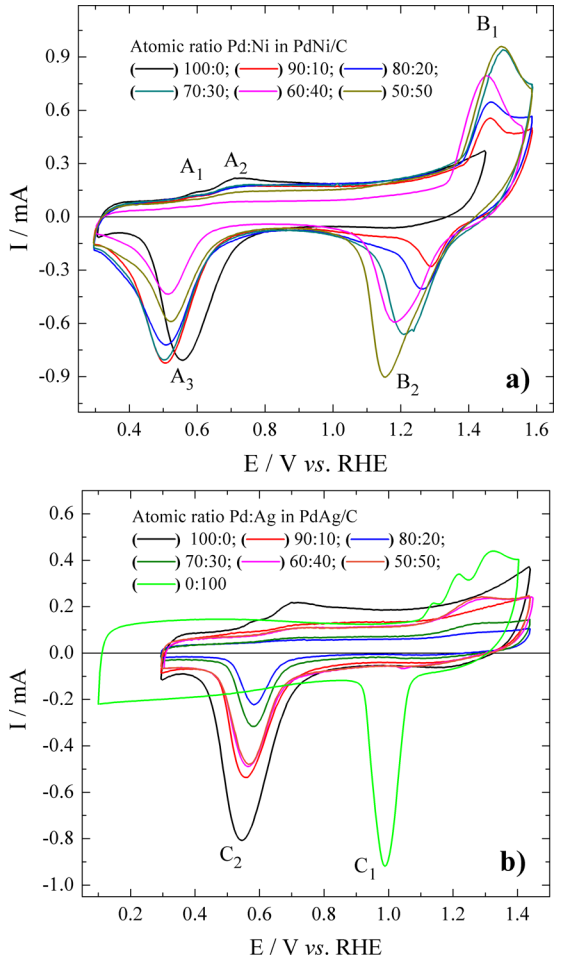

Figure 1. Cyclic voltammograms of (a) $Pd_xNi_{(100-x)}/C$ and (b) $Pd_xAg_{(100-x)}/C$ catalysts recorded at 50 mV s^{-1} in 0.1 mol L^{-1} NaOH electrolytic solution (20th cycle).

the reduction peak of PdO. A charge density of 424 μC cm^{-2} was associated with the reduction of the formed PdO monolayer.[76,77] The obtained value of 69 m^2 g_{Pd}^{-1} was found to be twice larger than that found by Simões et al.[77] for a Pd/C catalyst synthesized by the "water in oil" microemulsion method. Therefore, the synthesis of the nanomaterials by the BAE method appears as a promising process for obtaining electrocatalysts with high active surface areas. For the PdAg/C catalysts, the active surface areas were also calculated by integration of the reduction zones of PdO and Ag_2O. The complete method is described in section 3 of Supporting Information, Figure S2. A charge density of 420 μC cm^{-2} was associated to the reduction of the Ag_2O monolayer.[78] The obtained specific electrochemical surface areas (SECSA) values calculated for PdAg/C electrode materials by dividing the active surface area by the palladium weight were 47, 16, 34, 72, 72 m^2 g_{Pd}^{-1} for the $Pd_{90}Ag_{10}/C$, $Pd_{80}Ag_{20}/C$, $Pd_{70}Ag_{30}/C$, $Pd_{60}Ag_{40}/C$, and $Pd_{50}Ag_{50}/C$ compositions, respectively. In particular, it can be noticed that regarding the identical total metal loadings and particle size distributions obtained for the bimetallic catalysts, the low SECSA values reported herein for the $Pd_{80}Ag_{20}/C$ and $Pd_{70}Ag_{30}/C$ catalysts are quite unexpected. These values might nevertheless be explained by a lesser dispersion of metallic nanoparticles onto the supporting carbon for these two compositions. Because of the presence of $Ni(OH)_2$ species in the PdNi/C catalysts, it is not possible to evaluate their active surface areas.[38]

dx.doi.org/10.1021/cs400559d | ACS Catal. 2013, 3, 2403−2411

Electrochemical Activity toward Glycerol Oxidation. The glycerol electrooxidation reaction was considered during the positive variation of the electrode potential between 0.30−1.45 V vs RHE. The choice of the potential range was motivated by the possible application of catalysts in fuel cells or in electrosynthesis. The polarization curves are depicted in Figures 2a and b

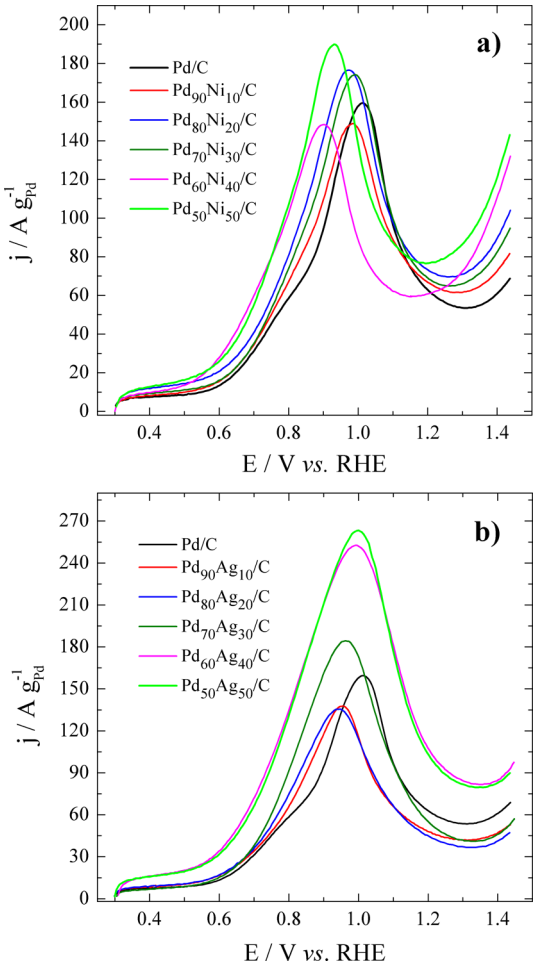

Figure 2. Polarization curves of glycerol oxidation on (a) $Pd_xNi_{(100-x)}/C$ and (b) $Pd_xAg_{(100-x)}/C$ catalysts at 50 mV s^{-1} in 0.1 mol L^{-1} NaOH electrolytic solution containing 0.1 mol L^{-1} of glycerol.

respectively for PdNi/C and PdAg/C catalysts. The catalytic activity was evaluated as a mass specific current (MSC, normalized with the mass of the most noble metal, Pd). The PdNi/C bimetallic catalysts exhibit good reaction kinetics at low potentials, as illustrated by the shift of the onset potential toward low potential values when compared with the Pd/C polarization curve. This improvement is attributed to a bifunctional mechanism of the oxidative desorption at low potential involving the transfer of OH^- species from the $Ni(OH)_2$ surface toward adsorbed organic molecules close to the palladium surface where the reaction takes place.[3,25] The forward oxidation current peak is attributed to the oxidation of freshly chemisorbed species coming from glycerol adsorption. Afterward, the current decreases because of the deactivation of the catalyst caused by the palladium surface oxidation. The reverse oxidation peak (Supporting Information, Figure S3) is associated with removal of carbonaceous species not completely oxidized in the forward scan.[26] One can also clearly observe the improvement of the catalytic activity of palladium with the increase of the silver content (Figure 2b), in agreement with results reported in the literature.[21,28] The promoting effect of the second metal has been explained by a bifunctional mechanism and/or electronic (ligand) effects.[21,75] According to Y. Wang et al.,[75] who have noticed the facility of removing CO from the PdAg/C catalysts surface, while Ag/C is not active in CO stripping, Ag promotes the removal of adsorbed CO or similar poisoning intermediates out of the surface of PdAg/C catalysts by a bifunctional mechanism. According to the d-band theory, when Ag is added into the structure of Pd, the d-band of Pd may be shifted up. As a result, more hydroxyls may be adsorbed at the catalyst surface and thus, more active sites are released.[21]

Electrolysis Experiments and HPLC Analysis. Electrolysis experiments were performed in alkaline solution for the different catalyst compositions. With the purpose of separating and identifying the final products of the glycerol electrooxidation in alkaline medium, the bulk solutions were analyzed by HPLC at different electrolysis times. Thus, a periodic PPE has been established to oxidize glycerol and chromatographically analyze the reaction products. The profile of the electrode potential as a function of the electrolysis time is reported in Supporting Information, Figure S5. For each cycle of electrolysis, the first potential plateau which was set to E_{ox} = 0.8 V vs RHE for 20 s, corresponds to the organic molecules' electrooxidation, and the second at E_{des} = 1.4 V vs RHE for 1 s, allows the regeneration of the electrode surface. The choice of the potential value 0.8 V RHE was done taking into consideration the prospective application in fuel cell devices. Indeed, for a fuel cell application the fundamental characteristics are the cell tension and the output power. The more interesting anodic material will be the one that provides the higher density current at low potential values. The chosen potential value is therefore a compromise between both aspects. The oxidation currents at E_{ox} = 0.8 V vs RHE (I_{ox}) and the quantity of electricity (Q_{ox}) are shown in Figures 3a and 3b, respectively, for selected catalysts. It can be noticed that whatever the anode catalyst the current intensity decreases fast during the first half hour before stabilization. As expected from previous reported results and evidenced by the obtained Q_{ox} values herein, the presence of Ag or Ni in the Pd-based catalysts improves the ability of the electrode material to oxidize glycerol. The $Pd_{70}Ag_{30}/C$ composition is of particular interest as it presents high oxidation current values and the smoothest stabilization curve. It should be noticed that all electrolysis experiments were performed during 4 h. However, after 2 h a slow and progressive decrease of the current intensity was observed which may be reasonably attributed to glycerol consumption and/or to oxygenated species production which are strongly adsorbed on the catalyst surface and cause its deactivation even with the desorption potential plateau.

Qualitative HPLC analyses are depicted in Figure 4 for different compositions of PdNi/C (Figure 4a) and PdAg/C (Figure 4b) nanocatalysts. The identified product distributions are given in Supporting Information, Figure S6 for three representative catalysts. The first important result is that all the catalysts are able to break the C−C bond of glycerol at ambient temperature. The second point is that the identified products were the same for the different studied compositions, the distributions of those products being slightly different. Indeed for all the compositions the major identified products were glycolic and glyceric acids. Figures 4c and d display glycerol molar conversions after 2 and 4 h of electrolysis for the different nickel or silver atomic compositions, respectively, of the PdM/C catalysts. It can be noticed that the $Pd_{80}Ni_{20}/C$ material exhibits

dx.doi.org/10.1021/cs400559d | ACS Catal. 2013, 3, 2403−2411

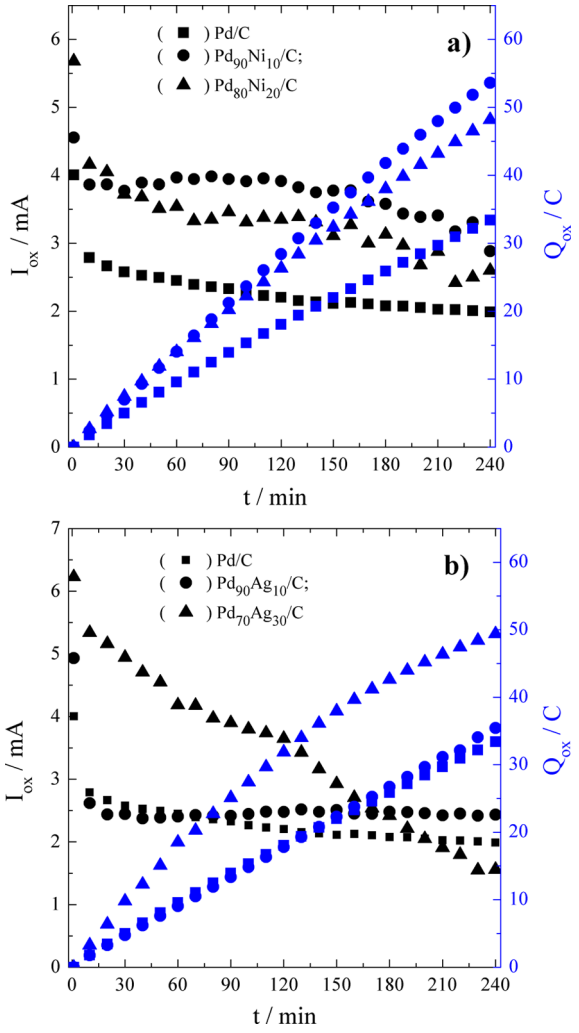

Figure 3. Evolution of the oxidation current (I_{ox}: black) and the quantity of electricity (Q_{ox}: blue) during the long-term electrolyses of glycerol (0.1 mol L^{-1}) in NaOH (0.1 mol L^{-1}) at 0.8 V vs RHE on (a) PdNi/C and (b) PdAg/C catalysts.

the best conversion (ca. 28.4% after 2 h of electrolysis and 31.3% after 4 h of electrolysis). These values are definitely low when compared with the ones reported in heterogeneous catalysis obtained in batch reactors, but they are, to our knowledge, the highest values reported for electrochemical glycerol conversion. In fact, Roquet and co-workers obtained the highest glycerol conversion of about 50% but after 48 h, instead of 4 h in the present work, of electrolysis at 0.79 V vs RHE on bulk platinum electrode (0.1 M NaOH + 0.1 M Glycerol).[1] More recently the Koper group also reported quantitative work, but their results did not show significant glycerol conversion.[11,46,49] The results reported herein are therefore very promising because they prove for the first time the potential conversion of glycerol on cheaper and more abundant metals than platinum. It should be pointed out that no correlation was found between the best glycerol conversion and the lower onset potential value.

It is commonly accepted that the oxidation of glycerol may imply two pathways involving glyceraldehyde and/or DHA (dihydroxyacetone). Nevertheless, both species, being unstable in alkaline medium because of the aldolization reaction,[79,80] could not be identified. Particularly the absence of glyceraldehyde can be explained by the Cannizzaro reaction which is a non Faradaic process that leads in alkaline solution to both glycerate and glycerol. So, glycerate, tartronate, glycolate, oxalate, and formate ions were the determined final products of glycerol electrooxidation in alkaline medium on PdM/C (M = Ag; Ni) catalysts. The presence of large amounts of glyceric acid indicates that the pathway involving glyceraldehyde is the most probable. However, in our operating conditions the hydroxypyruvic acid retention time is very close to that of tartronic acid and so we could not reach a conclusion about its presence in the analyzed solution. Furthermore, glycolic acid being a product of both proposed pathways, we cannot affirm as this stage that the glyceraldehyde pathway for the glycerol oxidation is the only one. So, complementary analyses by in situ FTIR experiments were undertaken to try to identify all the intermediates species.

In Situ Infrared Reflectance Spectroscopy Measurements. To get further insights on how glycerol is electrooxidized in alkaline medium on these nanoscale PdM/C materials, in situ spectroelectrochemical experiments have been undertaken. Figure 5 displays the single potential alteration infrared spectra (SPAIRS) obtained for Pd/C and $Pd_{60}Ni_{40}$/C catalysts during glycerol oxidation in alkaline medium. The first important result is that adsorbed CO is formed at low potential values (ca. 0.40 V vs RHE for Pd/C and 0.50 V vs RHE for PdNi/C) indicating the cleavage of C−C bond as reported in literature.[10,81] Indeed, the band at about 1887 cm^{-1} on Pd/C and 1895 cm^{-1} on $Pd_{60}Ni_{40}$/C is attributed to bridged CO (μ_2-(CO)) resulting from the rapid dissociative adsorption of glycerol at low potential values. For the PdAg/C catalysts (Supporting Information, Figure S7), the weak vibration band at 1888 cm^{-1} indicates the presence of bridged CO. Another important result is the evidence of CO_2 production on the different nanocatalysts (asymmetric stretching band at 2343 cm^{-1}).[47,48] This band appears at about 1.0 V vs RHE for bimetallic compositions and at about 1.1 V vs RHE for the monometallic composition and corresponds to the decrease of the absorbed CO band. According to Demarconnay et al.,[82] CO_2 appears in alkaline medium as soon as carbonate (1390−1420 cm^{-1} band)[48,82] could not be further formed because of the lack of OH^-. Jeffery and Camara[48] have proved by simple calculation in the thin layer (IR window-electrode interface) that the depletion of OH^- is enough to justify a sensible pH change during glycerol electrooxidation in alkaline medium. One can furthermore recognize the O−H stretching vibration band of carboxylic acid toward 3000 cm^{-1} confirming the acidification of the thin layer between the working electrode and the CaF_2 window.[83−85]

So far, it is herein clearly shown that (i) adsorbed CO is formed during the oxidation of glycerol for Pd-bases nanocatalysts, which results in poisoning of the catalysts at low potential values, and (ii) the main reaction products are glycolate and glycerate as evidenced by HPLC results and CO_2 as shown in the FTIR spectra. Based on the obtained spectra, we will undertake now to get further insights on the glycerol oxidation mechanism on Pd-based materials, and in particular we will attempt to identify the reaction intermediates. This will hopefully help us to reach conclusions about the preferential pathway and the crucial steps of the glycerol oxidation reaction in alkaline medium on Pd-based nanomaterials. The characteristic FTIR spectra of the different possible products or intermediates recorded in alkaline medium are depicted in Supporting Information, Figure S8 and will be used herein to reach conclusions on their presence in the electrolyte solution. So, for the Pd/C catalyst (Figure 5a) at low potential values (0.4−0.6 V vs RHE) the only identified intermediate is adsorbed CO. At higher potentials values (0.7−1.0 V vs RHE) evidence of the

dx.doi.org/10.1021/cs400559d | ACS Catal. 2013, 3, 2403−2411

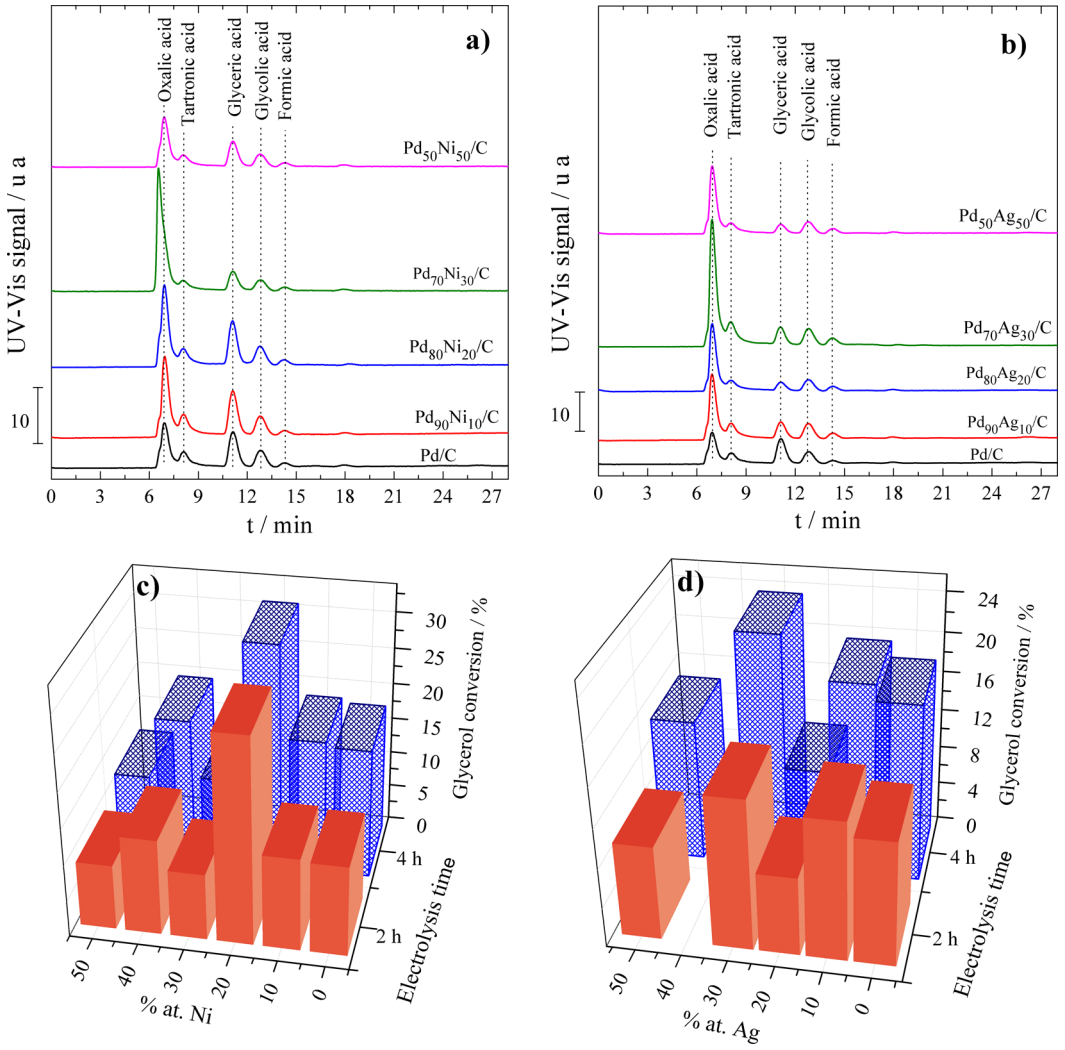

Figure 4. Chromatograms obtained from HPLC analysis after 4 h of electrolysis at 0.8 V vs RHE in 0.1 mol L^{-1} NaOH electrolytic solution containing 0.1 mol L^{-1} of glycerol for (a) PdNi/C and (b) PdAg/C catalysts. (Eluent: 3.3 mol L^{-1} H_2SO_4; injection: 20 μL; column Aminex HPX 87-H, 30 cm, at room temperature). (c, d) Glycerol conversion as a function of the molar compositions of the PdNi/C and PdAg/C catalysts, respectively, after 2 h and 4 h of electrolysis.

presence of other compounds could be found, namely, glycerate (1107 cm^{-1} and 1416 cm^{-1} bands), glycolate (1076 cm^{-1}, 1326 cm^{-1} and 1410 cm^{-1} bands), oxalate (sharp band at 1308 cm^{-1}), and formate (1350, 1382 cm^{-1}).[10,48,82,83] We cannot exclude at these potentials the formation of small amounts of tartronate and/or mesoxalate ions (characteristic IR bands at 1100, 1338, and 1438 cm^{-1}) in the thin layer electrolyte solution. It should be stated that the intense band at 1583 cm^{-1} is characteristic of different carboxylate ions and there also might be a contribution of the water bending vibration to this band.[47] Afterward, for potential values higher than 1.0 V vs RHE, CO_2 formation takes place while the amount of glycolate increases. A broad vibration band is also clearly visible between 1650 and 1720 cm^{-1} indicating the presence of adsorbed glyceraldehyde and carbonyl species.

Finally, the positive direction bands at 1050 and 2700 cm^{-1} are attributed to glycerol and OH^- consumption,[10,32,48,82] whereas the band at about 3700 cm^{-1} corresponds to water stretching vibrations.

The spectra obtained for the bimetallic catalysts (Figures 5b and Supporting Information, Figure S7) were similar to those obtained for the Pd/C material. The major difference occurs at low potential values for PdNi/C. Indeed, for potential values ranging from 0.3 to 0.7 V vs RHE two vibrational bands at 1595 and 1700 cm^{-1} are observed. The band at 1595 cm^{-1} can be assigned to different carboxylates such as glycerate and tartronate whereas the one at 1700 cm^{-1} is characteristic of adsorbed carbonyl species.

Based on these results we can therefore conclude that the pathway for the electrooxidation of glycerol on Pd-based materials in alkaline medium is the glyceraldehyde one.

An in situ IR study coupled with chronoamperometry experiments has also been performed. Chronoamperometry was carried out at 0.8 V vs RHE in the presence of 0.1 mol L^{-1} of glycerol. The obtained spectra are reported in Figure 6 for Pd/C and $Pd_{70}Ag_{30}$/C catalysts and in Supporting Information, Figure S9 for the $Pd_{60}Ni_{40}$/C composition. The absence of the band at 2343 cm^{-1} confirms the hypothesis that carbon dioxide is produced from $CO_{(ads)}$ at high potential values. In fact, the applied potential (0.8 V vs RHE) is not high enough to electrooxidize all adsorbed CO as shown by CO stripping experiments combined with FTIR spectroscopy measurements.[38] This is consistent with first Demarconnay et al.[82] and second Jeffery and Camara[48] observations. Another point is the

dx.doi.org/10.1021/cs400559d | ACS Catal. 2013, 3, 2403−2411

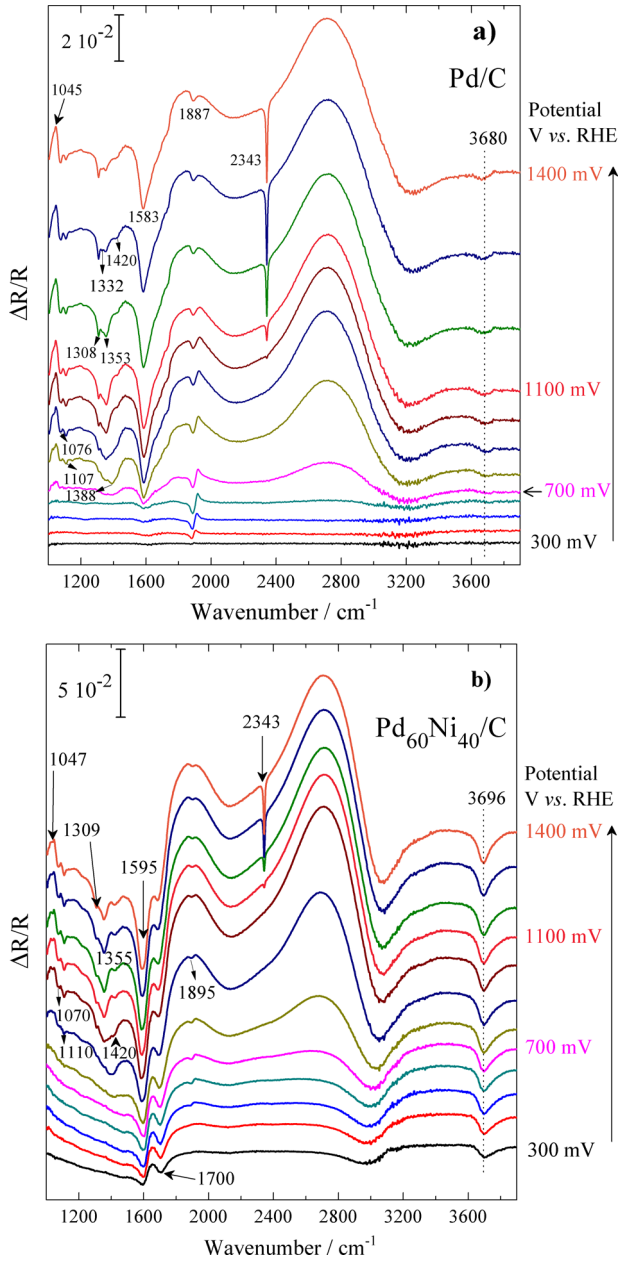

Figure 5. SPAIR spectra recorded in 0.1 mol L^{-1} NaOH electrolyte containing 0.1 mol L^{-1} of glycerol at 1 mV s^{-1} on (a) Pd/C and (b) $Pd_{60}Ni_{40}/C$ and catalysts at potentials ranging from 0.30 to 1.45 V vs RHE.

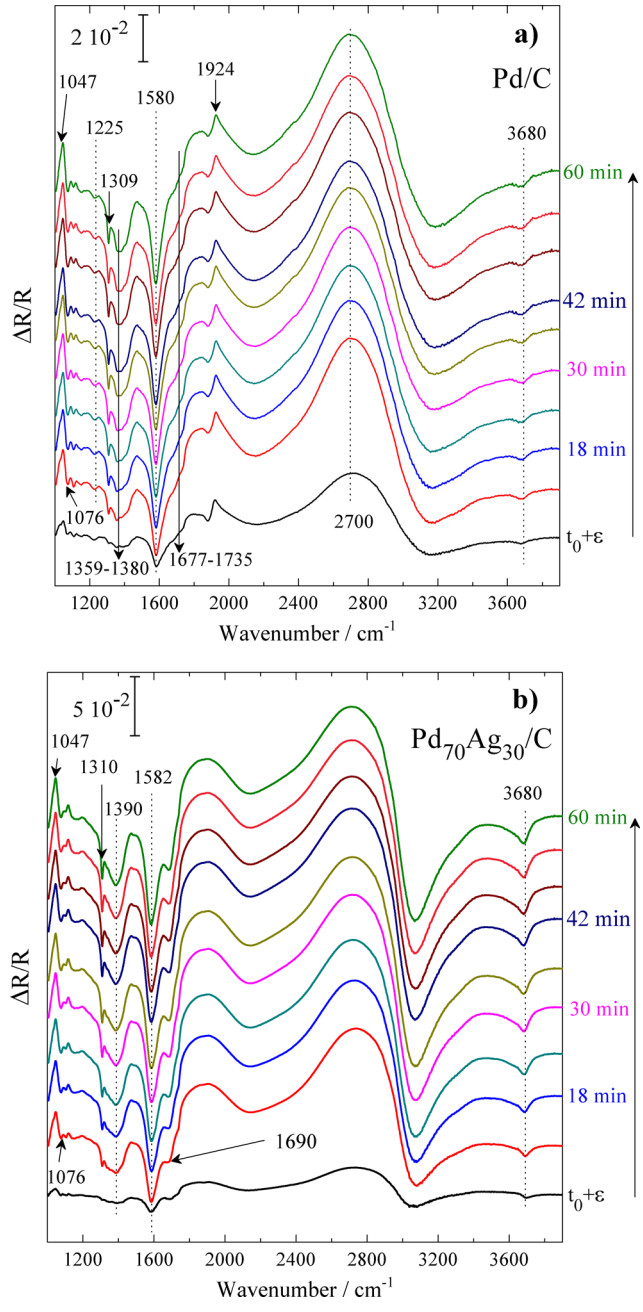

Figure 6. FTIR spectra recorded during chronoamperometry in 0.1 mol L^{-1} NaOH + 0.1 mol L^{-1} glycerol on (a) Pd/C and (b) $Pd_{70}Ag_{30}/C$ catalysts at 0.8 V vs RHE.

enhancement of some vibration bands that were hardly visible in the previous SPAIR spectra and that might be assigned to adsorbed species, confirming therefore the progressive poisoning of the catalysts. Indeed, the bands at 1225 and 1680 cm^{-1} have been assigned to adsorbed glyceraldehyde, whereas the band at about1380 cm^{-1} has been shown to be characteristic of adsorbed glycerate.[10] Chronoamperometry experiments coupled with in situ FTIR measurements confirm therefore the glyceraldehyde pathway for the glycerol electrooxidation in alkaline medium on Pd-based materials bringing to light adsorbed glyceraldehyde and glycerate as intermediates.

Glycerol Electrooxidation Scheme. According to HPLC analyses and in situ infrared measurements, we propose herein a scheme for glycerol electrooxidation in alkaline medium on the Pd-based nanocatalysts (Figure 7). Depending on the catalyst, it is possible to have other sequences, the composition of the catalyst and the potential of electrolysis being the keys of such processes. It is too early to talk about the reaction mechanism of glycerol electrooxidation. Indeed, the knowledge of the RDS (rate determining step(s)) is a prerequisite.

CONCLUSION

Nanoscale palladium−nickel or silver bimetallic electrocatalysts have been prepared by a synthetic route without the use of an organic compound as surfactant. We have shown by CV experiments the enhancement of the reaction kinetics in the low potential region for the different obtained bimetallic catalysts. The onset potential (ca. 0.4 V vs RHE) for the glycerol oxidation proves that one can replace platinum in the

dx.doi.org/10.1021/cs400559d | ACS Catal. 2013, 3, 2403−2411

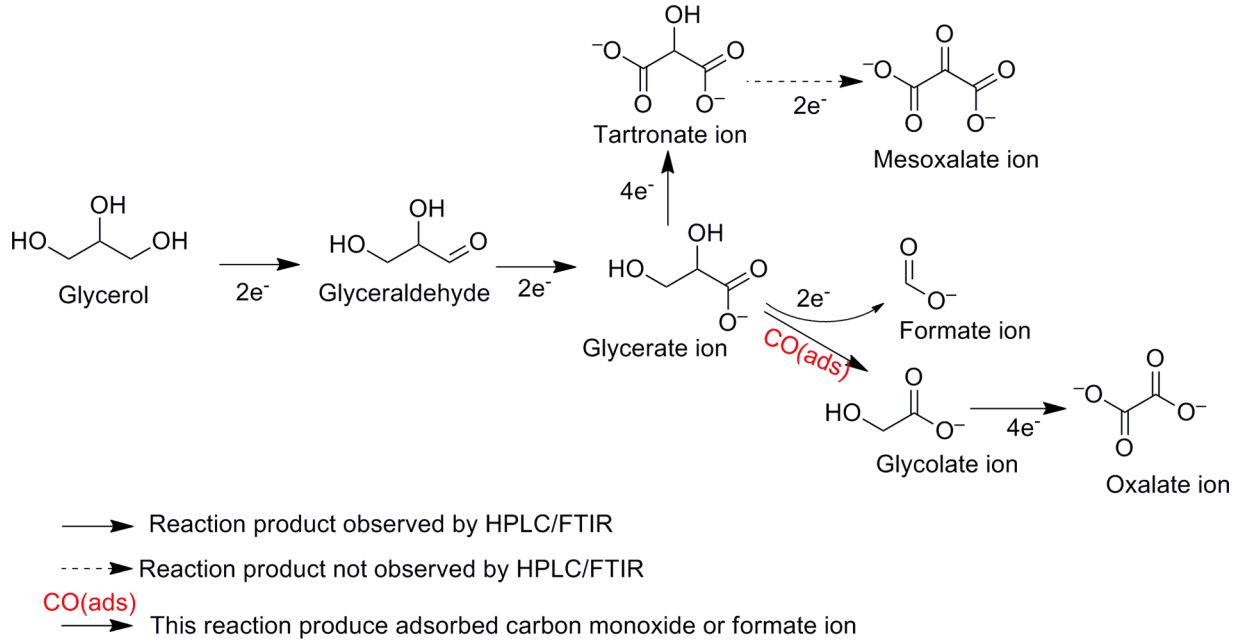

Figure 7. Proposed reaction scheme for glycerol electrooxidation on PdNi/C and PdAg/C nanocatalysts in alkaline medium. The dotted arrows indicate that the reaction product was not explicitly determined by HPLC.

electrocatalysts by palladium, which is at least 50 times more abundant on earth than platinum, combined with less expensive non noble metals (Ni, Ag) for obtaining better kinetics. By combining HPLC and in situ FTIR measurements, we were able to confirm that the glycerol electrooxidation on such catalysts involves glyceraldehyde as a reaction intermediate and that the major products are glycolate and glycerate ions. Furthermore carbon dioxide (2343 cm^{-1}) and carboxylic acid (3000 cm^{-1}) production during glycerol electrooxidation in alkaline medium (pH = 13) was also demonstrated, confirming the important change of pH nearby the electrode surface. The nature of the catalysts and the applied potential to perform electrolysis are therefore the important parameters that control the selectivity of the glycerol electrooxidation reaction toward the cogeneration of added value chemicals and the electric energy production in a fuel cell configuration.

■ ASSOCIATED CONTENT

Supporting Information

Electrochemical surface area evaluation, cyclic voltammogram of $Pd_{30}Ag_{70}/C$, effect of scan rate on glycerol electrooxidation, electrolysis current curves, product distributions, SPAIR spectra of the $Pd_{80}Ag_{20}/C$ catalyst, reference IR spectra, chronoamperommetry/IR spectra of $Pd_{60}Ni_{40}/C$. This material is available free of charge via the Internet at http://pubs.acs.org.

■ AUTHOR INFORMATION

Corresponding Author

*E-mail: claudia.gomes.de.morais@univ-poitiers.fr.

Notes

The authors declare no competing financial interest.

■ REFERENCES

(1) Roquet, L.; Belgsir, E. M.; Léger, J. M.; Lamy, C. *Electrochim. Acta* **1994**, *39*, 2387.
(2) Arechederra, R. L.; Treu, B. L.; Minteer, S. D. *J. Power Sources* **2007**, *173*, 156.
(3) Bianchini, C.; Shen, P. K. *Chem. Rev.* **2009**, *109*, 4183.
(4) Bambagioni, V.; Bianchini, C.; Marchionni, A.; Filippi, J.; Vizza, F.; Teddy, J.; Serp, P.; Zhiani, M. *J. Power Sources* **2009**, *190*, 241.
(5) Hong, P.; Luo, F.; Liao, S.; Zeng, J. *Int. J. Hydrogen Energy* **2011**, *36*, 8518.
(6) Steele, B. C. H.; Heinzel, A. *Nature* **2001**, *414*, 345.
(7) Matsuoka, K.; Iriyama, Y.; Abe, T.; Matsuoka, M.; Ogumi, Z. *J. Power Sources* **2005**, *150*, 27.
(8) Ilie, A.; Simoes, M.; Baranton, S.; Coutanceau, C.; Martemianov, S. *J. Power Sources* **2011**, *196*, 4965.
(9) Schäfer, H. J. *C. R. Chim.* **2011**, *14*, 745.
(10) Simões, M.; Baranton, S.; Coutanceau, C. *Appl. Catal., B* **2010**, *93*, 354.
(11) Kwon, Y.; Schouten, K. J. P.; Koper, M. T. M. *ChemCatChem* **2011**, *3*, 1176.
(12) Lamy, C.; Lima, A.; LeRhun, V.; Delime, F.; Coutanceau, C.; Léger, J. M. *J. Power Sources* **2002**, *105*, 283.
(13) Antolini, E. *J. Power Sources* **2007**, *170*, 1.
(14) Zhou, C.-H.; Beltramini, J. N.; Fan, Y.-X.; Lu, G. Q. *Chem. Soc. Rev.* **2008**, *37*, 527.
(15) Katryniok, B.; Kimura, H.; Skrzynska, E.; Girardon, J.-S.; Fongarland, P.; Capron, M.; Ducoulombier, R.; Mimura, N.; Paul, S.; Dumeignil, F. *Green Chem.* **2011**, *13*, 1960.
(16) Carrettin, S.; McMorn, P.; Johnston, P.; Griffin, K.; Kiely, C. J.; Hutchings, G. J. *Phys. Chem. Chem. Phys.* **2003**, *5*, 1329.
(17) Ketchie, W. C.; Murayama, M.; Davis, R. J. *J. Catal.* **2007**, *250*, 264.
(18) Zhang, Y.; Cui, X.; Shi, F.; Deng, Y. *Chem. Rev.* **2011**, *112*, 2467.
(19) Zhang, Z.; Xin, L.; Li, W. *Appl. Catal., B* **2012**, *119−120*, 40.
(20) Ksar, F. a.; Ramos, L.; Keita, B.; Nadjo, L.; Beaunier, P.; Remita, H. *Chem. Mater.* **2009**, *21*, 3677.
(21) Nguyen, S. T.; Law, H. M.; Nguyen, H. T.; Kristian, N.; Wang, S.; Chan, S. H.; Wang, X. *Appl. Catal., B* **2009**, *91*, 507.
(22) Singh, R. N.; Singh, A.; Anindita. *Carbon* **2009**, *47*, 271.
(23) Singh, R. N.; Singh, A.; Anindita. *Int. J. Hydrogen Energy* **2009**, *34*, 2052.
(24) Xu, J. B.; Zhao, T. S.; Shen, S. Y.; Li, Y. S. *Int. J. Hydrogen Energy* **2010**, *35*, 6490.
(25) Shen, S. Y.; Zhao, T. S.; Xu, J. B.; Li, Y. S. *J. Power Sources* **2010**, *195*, 1001.

(26) Zhao, Y.; Yang, X.; Tian, J.; Wang, F.; Zhan, L. *Int. J. Hydrogen Energy* **2010**, *35*, 3249.
(27) Lee, Y. W.; Kim, M.; Kim, Y.; Kang, S. W.; Lee, J.-H.; Han, S. W. *J. Phys. Chem. C* **2010**, *114*, 7689.
(28) Li, G.; Jiang, L.; Jiang, Q.; Wang, S.; Sun, G. *Electrochim. Acta* **2011**, *56*, 7703.
(29) Zhang, Z.; Xin, L.; Sun, K.; Li, W. *Int. J. Hydrogen Energy* **2011**, *36*, 12686.
(30) Simões, M.; Baranton, S.; Coutanceau, C. *ChemSusChem* **2012**, *5*, 2106.
(31) Lin, S.-C.; Chen, J.-Y.; Hsieh, Y.-F.; Wu, P.-W. *Mater. Lett.* **2011**, *65*, 215.
(32) Simões, M.; Baranton, S.; Coutanceau, C. *Appl. Catal., B* **2011**, *110*, 40.
(33) Mougenot, M.; Caillard, A.; Simoes, M.; Baranton, S.; Coutanceau, C.; Brault, P. *Appl. Catal., B* **2011**, *107*, 372.
(34) Nie, M.; Tang, H.; Wei, Z.; Jiang, S. P.; Shen, P. K. *Electrochem. Commun.* **2007**, *9*, 2375.
(35) Al-Odail, F. A.; Anastasopoulos, A.; Hayden, B. E. *Phys. Chem. Chem. Phys.* **2010**, *12*, 11398.
(36) Bianchini, C. In *Interfacial Phenomena in Electrocatalysis*; Vayenas, C. G., Ed.; Springer: New York, 2011; Vol. *51*, p 203.
(37) Ferreira, R. S., Jr.; Janete Giz, M.; Camara, G. A. *J. Electroanal. Chem.* **2013**, *697*, 15.
(38) Holade, Y.; Morais, C.; Arrii-Clacens, S.; Servat, K.; Napporn, T. W.; Kokoh, K. B. *Electrocatalysis* **2013**, *4*, 167.
(39) Pires, F. I.; Villullas, H. M. *Int. J. Hydrogen Energy* **2012**, *37*, 17052.
(40) Li, R.; Wei, Z.; Huang, T.; Yu, A. *Electrochim. Acta* **2011**, *56*, 6860.
(41) Liu, Z.; Zhang, X.; Hong, L. *Electrochem. Commun.* **2009**, *11*, 925.
(42) Ramos-Sánchez, G.; Yee-Madeira, H.; Solorza-Feria, O. *Int. J. Hydrogen Energy* **2008**, *33*, 3596.
(43) Martinez-Casillas, D. C.; Vazquez-Huerta, G.; Perez-Robles, J. F.; Solorza-Feria, O. *J. New Mater. Electrochem. Syst.* **2010**, *13*, 163.
(44) Bard, A. J.; Faulkner, L. R. *Electrochemical Methods: Fundamentals and Applications*, 2nd ed.; John Wiley & Son, Inc.: New York, 2001.
(45) Scholz, F. *Electroanalytical Methods: Guide to Experiments and Applications*; Springer-Verlag: Berlin, Germany, 2010.
(46) Kwon, Y.; Koper, M. T. M. *Anal. Chem.* **2010**, *82*, 5420.
(47) Gomes, J.; Tremiliosi-Filho, G. *Electrocatalysis* **2011**, *2*, 96.
(48) Jeffery, D. Z.; Camara, G. A. *Electrochem. Commun.* **2010**, *12*, 1129.
(49) Kwon, Y.; Birdja, Y.; Spanos, I.; Rodriguez, P.; Koper, M. T. M. *ACS Catal.* **2012**, *2*, 759.
(50) Fernández, P. S.; Martins, M. E.; Camara, G. A. *Electrochim. Acta* **2012**, *66*, 180.
(51) Alcaide, F.; Cabot, P.-L.; Brillas, E. *J. Power Sources* **2006**, *153*, 47.
(52) Tonda-Mikiela, P.; Napporn, T. W.; Morais, C.; Servat, K.; Chen, A.; Kokoh, K. B. *J. Electrochem. Soc.* **2012**, *159*, H828.
(53) Boutonnet, M.; Kizling, J.; Stenius, P.; Maire, G. *Colloids Surf.* **1982**, *5*, 209.
(54) Tojo, C.; Blanco, M. C.; Rivadulla, F.; López-Quintela, M. A. *Langmuir* **1997**, *13*, 1970.
(55) Solla-Gullón, J.; Rodes, A.; Montiel, V.; Aldaz, A.; Clavilier, J. *J. Electroanal. Chem.* **2003**, *554*−*555*, 273.
(56) Capek, I. *Adv. Colloid Interface Sci.* **2004**, *110*, 49.
(57) Guo, S.; Dong, S.; Wang, E. *ACS Nano* **2009**, *4*, 547.
(58) Carbone, L.; Cozzoli, P. D. *Nano Today* **2010**, *5*, 449.
(59) Wang, D.; Zhao, P.; Li, Y. *Sci. Rep.* **2011**, *1*, 37.
(60) Wang, Z.-L.; Yan, J.-M.; Wang, H.-L.; Ping, Y.; Jiang, Q. *Sci. Rep.* **2012**, *2*, 598.
(61) Ingert, D. In *Les nanosciences: 2. Nanomatériaux et nanochimie*, 2 ed.; Marcel Lahmani, C. B., Houdy, P., Eds.; Éditions Belin: Paris, France, 2012; p 463.
(62) Bard, A. J.; Faulkner, L. R. *Electrochemical Methods: Fundamentals and Applications*, 1st ed.; John Wiley & Son, Inc.: New York, 1980.
(63) Eklund, J. C.; Bond, A. M.; Alden, J. A.; Compton, R. G. In *Advances in Physical Organic Chemistry*; Bethell, D., Ed.; Academic Press: New York, 1999; Vol. *32*, p 1.
(64) Wang, J. *Analytical Electrochemistry*, 2nd ed.; John Wiley & Sons Inc.: New York, 2004.
(65) Wilson, M. S.; Valerio, J. A.; Gottesfeld, S. *Electrochim. Acta* **1995**, *40*, 355.
(66) Srinivasan, S.; Ticianelli, E. A.; Derouin, C. R.; Redondo, A. *J. Power Sources* **1988**, *22*, 359.
(67) Srinivasan, S.; Manko, D. J.; Koch, H.; Enayetullah, M. A.; Appleby, A. J. *J. Power Sources* **1990**, *29*, 367.
(68) Holze, R.; Ahn, J. *J. Membr. Sci.* **1992**, *73*, 87.
(69) Kokoh, K. B.; Léger, J. M.; Beden, B.; Huser, H.; Lamy, C. *Electrochim. Acta* **1992**, *37*, 1909.
(70) Corrigan, D. S.; Leung, L. W. H.; Weaver, M. J. *Anal. Chem.* **1987**, *59*, 2252.
(71) Beden, B.; Lamy, C. In *Spectroelectrochemistry*; Gale, R., Ed.; Springer: New York: 1988; p 189.
(72) Bae, I. T.; Xing, X.; Liu, C. C.; Yeager, E. *J. Electroanal. Chem. Interfacial Electrochem.* **1990**, *284*, 335.
(73) Tateishi, N.; Yahikozawa, K.; Nishimura, K.; Takasu, Y. *Electrochim. Acta* **1992**, *37*, 2427.
(74) Hu, C.-C.; Wen, T.-C. *Electrochim. Acta* **1995**, *40*, 495.
(75) Wang, Y.; Sheng, Z. M.; Yang, H.; Jiang, S. P.; Li, C. M. *Int. J. Hydrogen Energy* **2010**, *35*, 10087.
(76) Grden, M.; Lukaszewski, M.; Jerkiewicz, G.; Czerwinski, A. *Electrochim. Acta* **2008**, *53*, 7583.
(77) Simões, M.; Baranton, S.; Coutanceau, C. *J. Phys. Chem. C* **2009**, *113*, 13369.
(78) Maheswari, S.; Sridhar, P.; Pitchumani, S. *Electrocatalysis* **2012**, *3*, 13.
(79) Yaylayan, V. A.; Ismail, A. A. *Carbohydr. Res.* **1995**, *276*, 253.
(80) A. Yaylayan, V.; Harty-Majors, S.; A. Ismail, A. *Carbohydr. Res.* **1999**, *318*, 20.
(81) Sun, S.-G. In *Electrocatalysis*; Lipkowski, J., Ross, P. N., Eds.; Wiley-VCH, Inc.: New York, 1998; p 243.
(82) Demarconnay, L.; Brimaud, S.; Coutanceau, C.; Léger, J. M. *J. Electroanal. Chem.* **2007**, *601*, 169.
(83) Pouchert, C. J. *The Aldrich Library of Infrared Spectra*, 3rd ed.; Aldrich Chemical Company, Inc.: Milwaukee, WI, 1981.
(84) E. Bourguet, C. A. *Les techniques de laboratoire: Purification et analyse des composés organiques*; Edition Ellipses, THECHNOSUP: Paris, France, 2008.
(85) Orozco, G.; Pérez, M. C.; Rincón, A.; Gutiérrez, C. *J. Electroanal. Chem.* **2000**, *495*, 71.